

THE UNIVERSITY OF WARWICK

Original citation:

LHCb Collaboration (Including: Back, John J., Craik, Daniel, Dossett, D., Gershon, Timothy J., Kreps, Michal, Latham, Thomas, Pilar, T., Poluektov, Anton, Reid, Matthew M., Silva Coutinho, R., Wallace, C., Whitehead, M. (Mark) and Williams, M. P.). (2013) Model-independent search for CP violation in $D^0 \rightarrow K^- K^+ \pi^- \pi^+$ and $D^0 \rightarrow \pi^- \pi^+ \pi^+ \pi^-$ decays. Physics Letters B, Volume 726 (Number 4–5). ISSN 0370-2693

Permanent WRAP url:

<http://wrap.warwick.ac.uk/57934>

Copyright and reuse:

The Warwick Research Archive Portal (WRAP) makes this work of researchers of the University of Warwick available open access under the following conditions.

This article is made available under the Creative Commons Attribution 3.0 (CC BY 3.0) license and may be reused according to the conditions of the license. For more details see: <http://creativecommons.org/licenses/by/3.0/>

A note on versions:

The version presented in WRAP is the published version, or, version of record, and may be cited as it appears here.

For more information, please contact the WRAP Team at: publications@warwick.ac.uk



<http://wrap.warwick.ac.uk>



Model-independent search for CP violation in $D^0 \rightarrow K^-K^+\pi^-\pi^+$ and $D^0 \rightarrow \pi^-\pi^+\pi^+\pi^-$ decays[☆]



LHCb Collaboration

ARTICLE INFO

Article history:

Received 15 August 2013
 Received in revised form 5 September 2013
 Accepted 5 September 2013
 Available online 12 September 2013
 Editor: W.-D. Schlatter

ABSTRACT

A search for CP violation in the phase-space structures of D^0 and \bar{D}^0 decays to the final states $K^-K^+\pi^-\pi^+$ and $\pi^-\pi^+\pi^+\pi^-$ is presented. The search is carried out with a data set corresponding to an integrated luminosity of 1.0 fb^{-1} collected in 2011 by the LHCb experiment in pp collisions at a centre-of-mass energy of 7 TeV. For the $K^-K^+\pi^-\pi^+$ final state, the four-body phase space is divided into 32 bins, each bin with approximately 1800 decays. The p -value under the hypothesis of no CP violation is 9.1%, and in no bin is a CP asymmetry greater than 6.5% observed. The phase space of the $\pi^-\pi^+\pi^+\pi^-$ final state is partitioned into 128 bins, each bin with approximately 2500 decays. The p -value under the hypothesis of no CP violation is 41%, and in no bin is a CP asymmetry greater than 5.5% observed. All results are consistent with the hypothesis of no CP violation at the current sensitivity.

© 2013 CERN. Published by Elsevier B.V. All rights reserved.

1. Introduction

Standard Model predictions for the magnitude of CP violation (CPV) in charm meson decays are generally of $\mathcal{O}(10^{-3})$ [1,2], although values up to $\mathcal{O}(10^{-2})$ cannot be ruled out [3,4]. The size of CPV can be significantly enhanced in new physics models [5,6], making charm transitions a promising area to search for new physics. Previous searches for CPV in charm decays caused a large interest in the community [7–9] and justify detailed searches for CPV in many different final states. Direct CPV can occur when at least two amplitudes interfere with strong and weak phases that each differ from one another. Singly-Cabibbo-suppressed charm hadron decays, where both tree processes and electroweak loop processes can contribute, are promising channels with which to search for CPV. The rich structure of interfering amplitudes makes four-body decays ideal to perform such searches.

The phase-space structures of the $D^0 \rightarrow K^-K^+\pi^-\pi^+$ and $D^0 \rightarrow \pi^-\pi^+\pi^+\pi^-$ decays¹ are investigated for localised CPV in a manner that is independent of an amplitude model of the D^0 meson decay. The Cabibbo-favoured $D^0 \rightarrow K^-\pi^+\pi^+\pi^-$ decay, where no significant direct CPV is expected within the Standard Model, is used as a control channel. A model-dependent search for CPV in $D^0 \rightarrow K^-K^+\pi^-\pi^+$ was previously carried out by the CLEO Collaboration [10] with a data set of approximately 3000 signal decays, where no evidence for CPV was observed. This analysis is carried out on a data set of approximately 5.7×10^4 $D^0 \rightarrow K^-K^+\pi^-\pi^+$ decays and 3.3×10^5 $D^0 \rightarrow \pi^-\pi^+\pi^+\pi^-$ decays. The data set is

based on an integrated luminosity of 1.0 fb^{-1} of pp collisions with a centre-of-mass energy of 7 TeV, recorded by the LHCb experiment during 2011. The analysis is based on D^0 mesons produced in $D^{*+} \rightarrow D^0\pi^+$ decays. The charge of the soft pion (π^+) identifies the flavour of the meson at production. The phase space is partitioned into N_{bins} bins, and the significance of the difference in population between CP conjugate decays for each bin is calculated as

$$S_{CP}^i = \frac{N_i(D^0) - \alpha N_i(\bar{D}^0)}{\sqrt{\alpha(\sigma_i^2(D^0) + \sigma_i^2(\bar{D}^0))}}, \quad \alpha = \frac{\sum_i N_i(D^0)}{\sum_i N_i(\bar{D}^0)}, \quad (1)$$

where N_i is the number of signal decays in bin i , and σ_i is the associated uncertainty in the number of signal decays in bin i [11]. The normalisation constant α removes global production and detection differences between D^{*+} and D^{*-} decays.

In the absence of any asymmetry, S_{CP} is Gaussian distributed with a mean of zero and a width of one. A significant variation from a unit Gaussian distribution indicates the presence of an asymmetry. The sum of squared S_{CP} values is a χ^2 statistic,

$$\chi^2 = \sum_i (S_{CP}^i)^2,$$

with $N_{\text{bins}} - 1$ degrees of freedom, from which a p -value is calculated. Previous analyses of three-body D meson decays have employed similar analysis techniques [12,13].

2. Detector

The LHCb detector [14] is a single-arm forward spectrometer covering the pseudorapidity range $2 < \eta < 5$, designed for

[☆] © CERN for the benefit of the LHCb Collaboration.

¹ Unless otherwise specified, inclusion of charge-conjugate processes is implied.

the study of particles containing b or c quarks. The detector includes a high-precision tracking system consisting of a silicon-strip vertex detector surrounding the pp interaction region, a large-area silicon-strip detector located upstream of a dipole magnet with a vertically oriented magnetic field and bending power of about 4 Tm, and three stations of silicon-strip detectors and straw drift tubes placed downstream. To alleviate the impact of charged particle–antiparticle detection asymmetries, the magnetic field polarity is switched regularly, and data are taken in each polarity. The two magnet polarities are henceforth referred to as “magnet up” and “magnet down”. The combined tracking system provides momentum measurement with relative uncertainty that varies from 0.4% at 5 GeV/c to 0.6% at 100 GeV/c, and impact parameter resolution of 20 μm for tracks with high transverse momentum. Charged hadrons are identified with two ring-imaging Cherenkov (RICH) detectors [15]. Photon, electron, and hadron candidates are identified by a calorimeter system consisting of scintillating-pad and preshower detectors, an electromagnetic calorimeter, and a hadronic calorimeter. Muons are identified by a system composed of alternating layers of iron and multiwire proportional chambers. The trigger consists of a hardware stage, based on information from the calorimeter and muon systems, followed by a software stage [16]. Events are required to pass both hardware and software trigger levels. The software trigger optimised for the reconstruction of four-body hadronic charm decays requires a four-track secondary vertex with a scalar sum of the transverse momenta, p_T , of the tracks greater than 2 GeV/c. At least two tracks are required to have $p_T > 500$ MeV/c and momentum, p , greater than 5 GeV/c. The remaining two tracks are required to have $p_T > 250$ MeV/c and $p > 2$ GeV/c. A requirement is also imposed on the χ^2 of the impact parameter (χ_{IP}^2) of the remaining two tracks with respect to any primary interaction to be greater than 10, where χ_{IP}^2 is defined as the difference in χ^2 of a given primary vertex reconstructed with and without the considered track.

3. Selection

Candidate D^0 decays are reconstructed from combinations of pion and kaon candidate tracks. The D^0 candidates are required to have $p_T > 3$ GeV/c. The D^0 decay products are required to have $p > 3$ GeV/c and $p_T > 350$ MeV/c. The D^0 decay products are required to form a vertex with a χ^2 per degree of freedom (χ^2/ndf) less than 10 and a maximum distance of closest approach between any pair of D^0 decay products less than 0.12 mm. The RICH system is used to distinguish between kaons and pions when reconstructing the D^0 candidate. The D^{*+} candidates are reconstructed from D^0 candidates combined with a track with $p_T > 120$ MeV/c. Decays are selected with candidate D^0 mass, $m(hhhh)$, of $1804 < m(hhhh) < 1924$ MeV/c², where the notation $m(hhhh)$ denotes the invariant mass of any of the considered final states; specific notations are used where appropriate. The difference, Δm , in the reconstructed D^{*+} mass and $m(hhhh)$ for candidate decays is required to be $137.9 < \Delta m < 155.0$ MeV/c². The decay vertex of the D^* is constrained to coincide with the primary vertex [17].

Differences in D^{*+} and D^{*-} meson production and detection efficiencies can introduce asymmetries across the phase-space distributions of the D^0 decay. To ensure that the soft pion is detected in the central region of the detector, fiducial cuts on its momentum are applied, as in Ref. [9]. The D^0 and \bar{D}^0 candidates are weighted by removing events so that they have same transverse momentum and pseudorapidity distributions. To further cancel detection asymmetries the data set is selected to contain equal quantities of data collected with each magnetic field polarity. Events are randomly removed from the largest subsample of the two magnetic field polarity configurations.

Each data sample is investigated for background contamination. The reconstructed D^0 mass is searched for evidence of backgrounds from misreconstructed D^0 decays in which K/π misidentification has occurred. Candidates in which only a single final-state particle is misidentified are reconstructed outside the $m(hhhh)$ signal range. No evidence for candidates with two, three, or four K/π misidentifications is observed. Charm mesons from b -hadron decays are strongly suppressed by the requirement that the D^0 candidate originates from a primary vertex. This source of background is found to have a negligible contribution.

4. Method

Fig. 1 shows the $m(hhhh)$ and Δm distributions for D^0 candidate decays to the final states $K^-K^+\pi^-\pi^+$, $\pi^-\pi^+\pi^+\pi^-$, and $K^-\pi^+\pi^+\pi^-$, for data taken with magnet up polarity. The distributions for \bar{D}^0 candidates and data taken with magnet down polarity are consistent with the distributions shown. Two-dimensional unbinned likelihood fits are made to the $m(hhhh)$ and Δm distributions to separate signal and background contributions. Each two-dimensional $[m(hhhh), \Delta m]$ distribution includes contributions from the following sources: signal D^0 mesons from D^{*+} decays, which peak in both $m(hhhh)$ and Δm ; combinatorial background candidates, which do not peak in either $m(hhhh)$ or Δm ; background candidates from an incorrect association of a soft pion with a real D^0 meson, which peak in $m(hhhh)$ and not in Δm ; incorrectly reconstructed $D_s^+ \rightarrow K^-K^+\pi^-\pi^+\pi^+$ decays, which peak at low values of $m(hhhh)$ but not in Δm ; and misreconstructed $D^0 \rightarrow K^-\pi^+\pi^-\pi^+\pi^0$ decays, which have broad distributions in both $m(hhhh)$ and Δm . The signal distribution is described by a Crystal Ball function [18] plus a Gaussian function, with a shared peak value, in $m(hhhh)$ and Johnson function [19] of the form

$$J(\Delta m) \propto \frac{\exp(-\frac{1}{2}[\gamma + \delta \sinh^{-1}(\frac{\Delta m - \mu}{\sigma})]^2)}{\sqrt{1 + (\frac{\Delta m - \mu}{\sigma})^2}} \quad (2)$$

in Δm . The combinatorial background is modelled with a first-order polynomial in $m(hhhh)$, and the background from D^0 candidates each associated with a random soft pion is modelled by a Gaussian distribution in $m(hhhh)$. Both combinatorial and random soft pion backgrounds are modelled with a function of the form

$$f(\Delta m) = [(\Delta m - \Delta m_0) + p_1(\Delta m - \Delta m_0)^2]^a \quad (3)$$

in Δm , where Δm_0 is the kinematic threshold (fixed to the pion mass), and the parameters p_1 and a are allowed to float.

Partially reconstructed $D_s^+ \rightarrow K^-K^+\pi^-\pi^+\pi^+$ decays, where a single pion is not reconstructed, are investigated with simulated decays. This background is modelled with a Gaussian distribution in $m(hhhh)$ and with a function $f(\Delta m)$ as defined in Eq. (3). Misreconstructed $D^0 \rightarrow K^-\pi^+\pi^-\pi^+\pi^0$ decays where a single K/π misidentification has occurred and where the π^0 is not reconstructed are modelled with a shape from simulated decays. Other potential sources of background are found to be negligible.

For each two-dimensional $[m(hhhh), \Delta m]$ distribution a fit is first performed to the background region, $139 < \Delta m < 143$ MeV/c² or $149 < \Delta m < 155$ MeV/c², to obtain the shapes of the combinatorial and soft pion backgrounds. The Δm components of these shapes are fixed and a two-dimensional fit is subsequently performed simultaneously over four samples (D^0 magnet up, \bar{D}^0 magnet up, D^0 magnet down, and \bar{D}^0 magnet down). The peak positions and widths of the signal shapes and all yields are allowed to vary independently for each sample, whilst all other parameters are shared among the four samples. A signal yield of 5.7×10^4

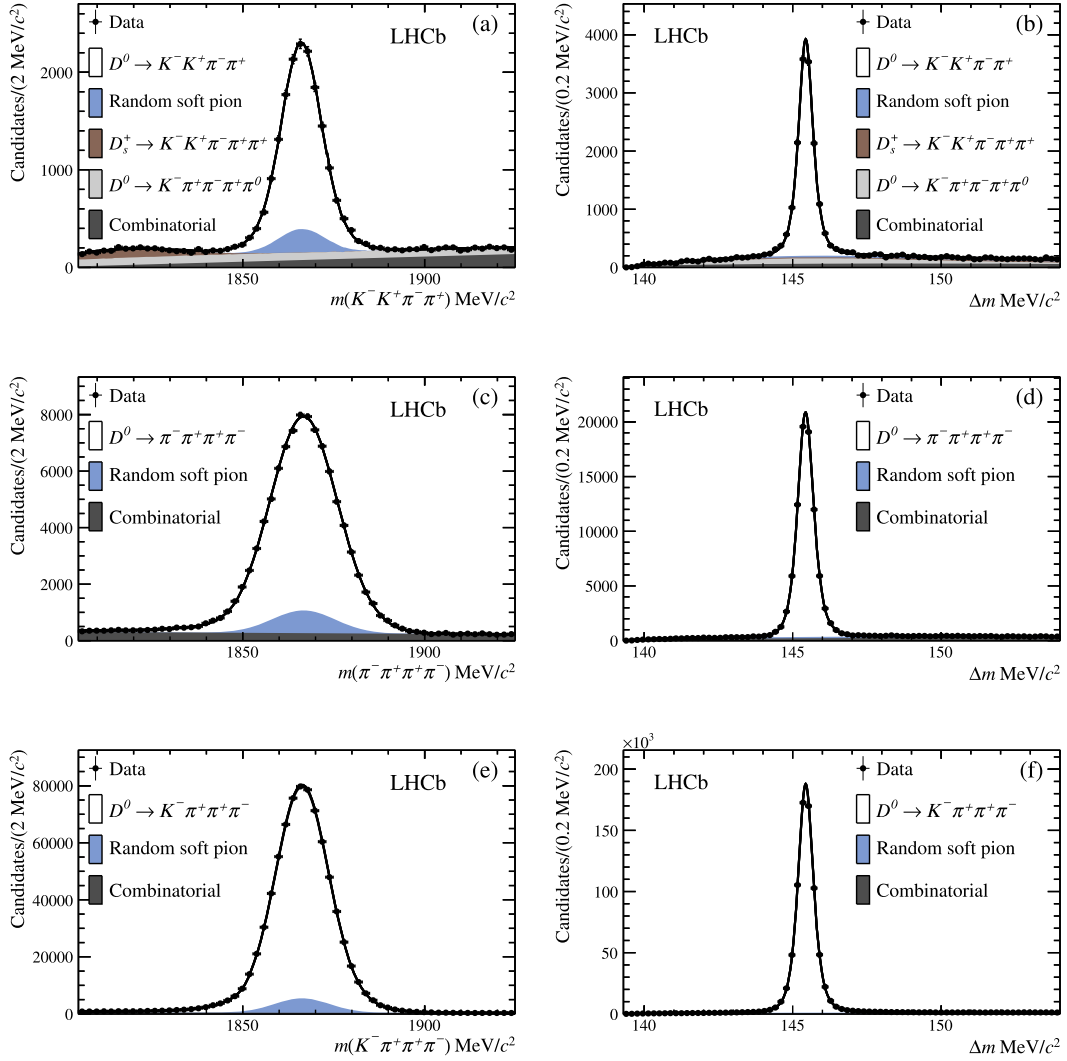


Fig. 1. Distributions of (a), (c), (e) $m(hhhh)$ and (b), (d), (f) Δm for (a), (b) $D^0 \rightarrow K^- K^+ \pi^- \pi^+$, (c), (d) $D^0 \rightarrow \pi^- \pi^+ \pi^+ \pi^-$, and (e), (f) $D^0 \rightarrow K^- \pi^+ \pi^+ \pi^-$ candidates for magnet up polarity. Projections of the two-dimensional fits are overlaid, showing the contributions for signal, combinatorial background, and random soft pion background. The contributions from $D^0 \rightarrow K^- \pi^+ \pi^- \pi^+ \pi^0$ and $D_s^+ \rightarrow K^- K^+ \pi^- \pi^+ \pi^+$ contamination are also shown for the $D^0 \rightarrow K^- K^+ \pi^- \pi^+$ sample.

$D^0 \rightarrow K^- K^+ \pi^- \pi^+$, 3.3×10^5 $D^0 \rightarrow \pi^- \pi^+ \pi^+ \pi^-$, and 2.9×10^6 $D^0 \rightarrow K^- \pi^+ \pi^+ \pi^-$ decays is extracted from the two-dimensional fits. The *sPlot* statistical method [20] is used to obtain background subtracted phase-space distributions for D^0 decays to the final states $K^- K^+ \pi^- \pi^+$, $\pi^- \pi^+ \pi^+ \pi^-$, and $K^- \pi^+ \pi^+ \pi^-$. The *sWeights* are calculated from the likelihood fits to the two-dimensional $[m(hhhh), \Delta m]$ distributions.

The phase space of a spin-0 decay to four pseudoscalars can be described with five invariant mass-squared combinations: $s(1, 2)$, $s(2, 3)$, $s(1, 2, 3)$, $s(2, 3, 4)$, and $s(3, 4)$, where the indices 1, 2, 3, and 4 correspond to the decay products of the D^0 meson following the ordering of the decay definitions. The ordering of identical final-state particles is randomised.

The rich amplitude structures are visible in the invariant mass-squared distributions for D^0 and \bar{D}^0 decays to the final states $K^- K^+ \pi^- \pi^+$ and $\pi^- \pi^+ \pi^+ \pi^-$, shown in Figs. 2 and 3, respectively. The momenta of the final-state particles are calculated with the decay vertex of the D^* constrained to coincide with the primary vertex and the mass of the D^0 candidates constrained to the world average value of $1864.86 \text{ MeV}/c^2$ [22].

An adaptive binning algorithm is devised to partition the phase space of the decay into five-dimensional hypercubes. The bins are

defined such that each contains a similar number of candidates, resulting in fine bins around resonances and coarse bins across sparsely populated regions of phase space.

For each phase-space bin, S_{CP}^i , defined in Eq. (1), is calculated. The number of signal events in bin i , N_i , is calculated as the sum of the signal weights in bin i and σ_i^2 is the sum of the squared weights. The normalisation factor, α , is calculated as the ratio of the sum of the weights for D^0 candidates and the sum of the weights for \bar{D}^0 candidates and is 1.001 ± 0.008 , 0.996 ± 0.003 , and 0.998 ± 0.001 for the final states $K^- K^+ \pi^- \pi^+$, $\pi^- \pi^+ \pi^+ \pi^-$, and $K^- \pi^+ \pi^+ \pi^-$, respectively.

5. Production and instrumental asymmetries

Checks for remaining production or reconstruction asymmetries are carried out by comparing the phase-space distributions from a variety of data sets designed to test particle/antiparticle detection asymmetries and “left/right” detection asymmetries. The “left” direction is defined as the bending direction of a positively charged particle with the magnet up polarity. Asymmetries in the background are studied with weighted background candidates and mass sidebands.

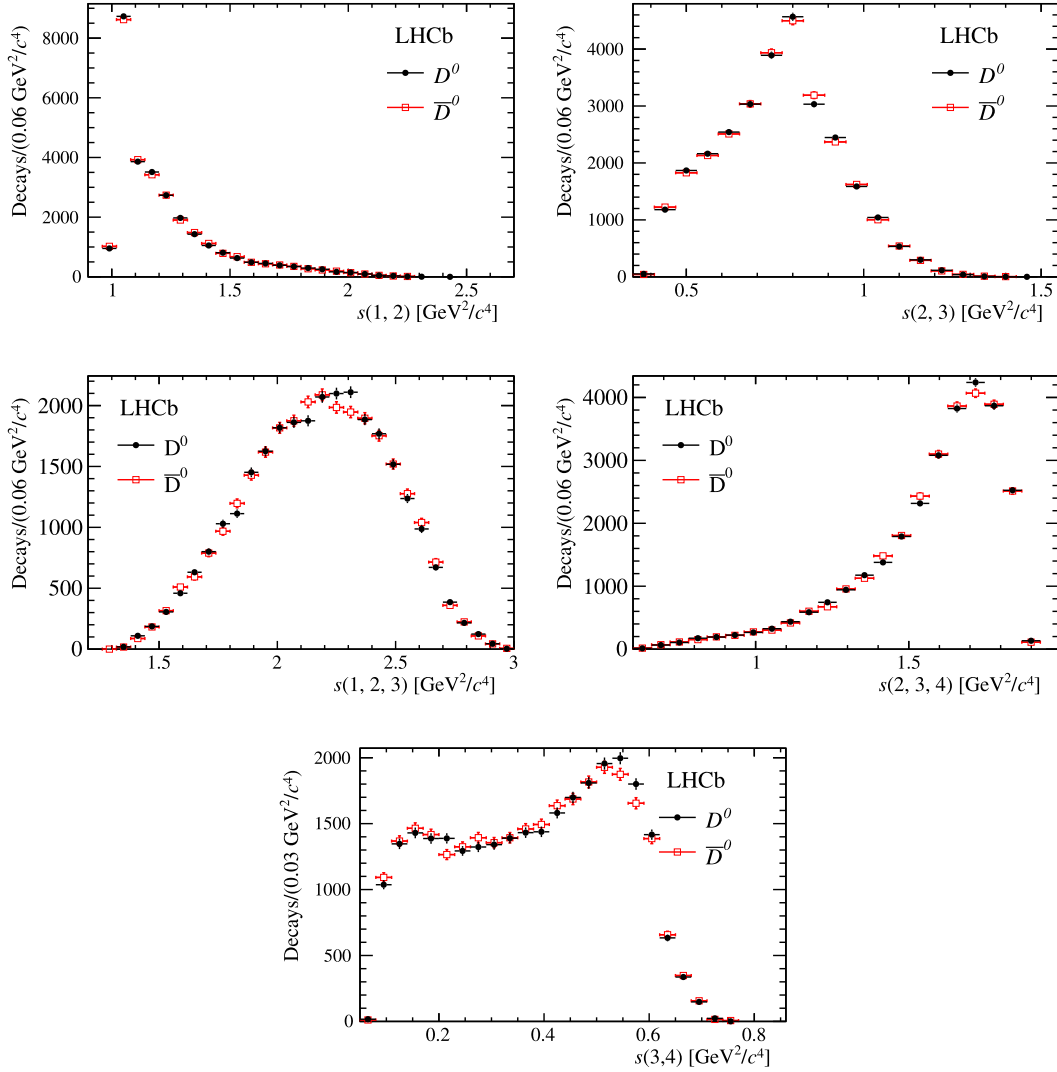


Fig. 2. Invariant mass-squared distributions for D^0 meson (black, closed circles) and \bar{D}^0 meson (red, open squares) decays to the final state $K^-K^+\pi^-\pi^+$. The invariant mass-squared combinations $s(1, 2)$, $s(2, 3)$, $s(1, 2, 3)$, $s(2, 3, 4)$, and $s(3, 4)$ correspond to $s(K^-, K^+)$, $s(K^+, \pi^-)$, $s(K^-, K^+, \pi^-)$, $s(K^+, \pi^-, \pi^+)$, and $s(\pi^-, \pi^+)$, respectively for the D^0 mode. The charge conjugate is taken for the \bar{D}^0 mode. The phase-space distribution of the $D^0 \rightarrow K^-K^+\pi^-\pi^+$ decay is expected to be dominated by the quasi-two-body decay $D^0 \rightarrow \phi\rho^0$ with additional contributions from $D^0 \rightarrow K_1(1270)^\pm K^\mp$ and $D^0 \rightarrow K^*(1410)^\pm K^\mp$ decays [10]. (For interpretation of the references to colour in this figure legend, the reader is referred to the web version of this Letter.)

Left/right asymmetries in detection efficiencies are investigated by comparing the phase-space distributions of D^0 candidates in data taken with opposite magnet polarities, thus investigating the same flavour particles in opposite sides of the detector. Particle/antiparticle asymmetries are studied with the control channel $D^0 \rightarrow K^-\pi^+\pi^+\pi^-$. The weighting based on p_T and pseudorapidity of the D^0 candidate and the normalisation across the phase space of the D^0 decay cancel the K^+/K^- detection asymmetry in this control channel. The phase-space distribution of D^0 decays from data taken with one magnet polarity is compared with that of \bar{D}^0 decays from data taken with the opposite magnet polarity, for any sources of particle/antiparticle detection asymmetry, localised across the phase space of the D^0 decay.

The weighted distributions for each of the background components in the two-dimensional fits are investigated for asymmetries in $D^0 \rightarrow K^-K^+\pi^-\pi^+$, $D^0 \rightarrow \pi^-\pi^+\pi^+\pi^-$, and $D^0 \rightarrow K^-\pi^+\pi^+\pi^-$ candidates. The Δm and $m(hhhh)$ sidebands are also investigated to identify sources of asymmetry.

The sensitivity to asymmetries is limited by the sample size, so S_{CP} is calculated only with statistical uncertainties.

6. Sensitivity studies

Pseudo-experiments are carried out to investigate the dependence of the sensitivity on the number of bins. Each pseudo-experiment is generated with a sample size comparable to that available in data.

Decays are generated with MINT, a software package for amplitude analysis of multi-body decays that has also been used by the CLEO Collaboration [10]. A sample of $D^0 \rightarrow K^-K^+\pi^-\pi^+$ decays is generated according to the amplitude model reported by CLEO [10], and $D^0 \rightarrow \pi^-\pi^+\pi^+\pi^-$ decays are generated according to the amplitude model from the FOCUS Collaboration [21]. Phase and magnitude differences between D^0 and \bar{D}^0 decays are introduced. Fig. 4 shows the S_{CP} distributions for a typical pseudo-experiment in which no CPV is present and for a typical pseudo-experiment with a phase difference of 10° between $D^0 \rightarrow a_1(1260)^+\pi^-$ and $\bar{D}^0 \rightarrow a_1(1260)^-\pi^+$ decays.

Based on the results of the sensitivity study, a partition with 32 bins, each with approximately 1800 signal events, is chosen for $D^0 \rightarrow K^-K^+\pi^-\pi^+$ decays while a partition with 128 bins,

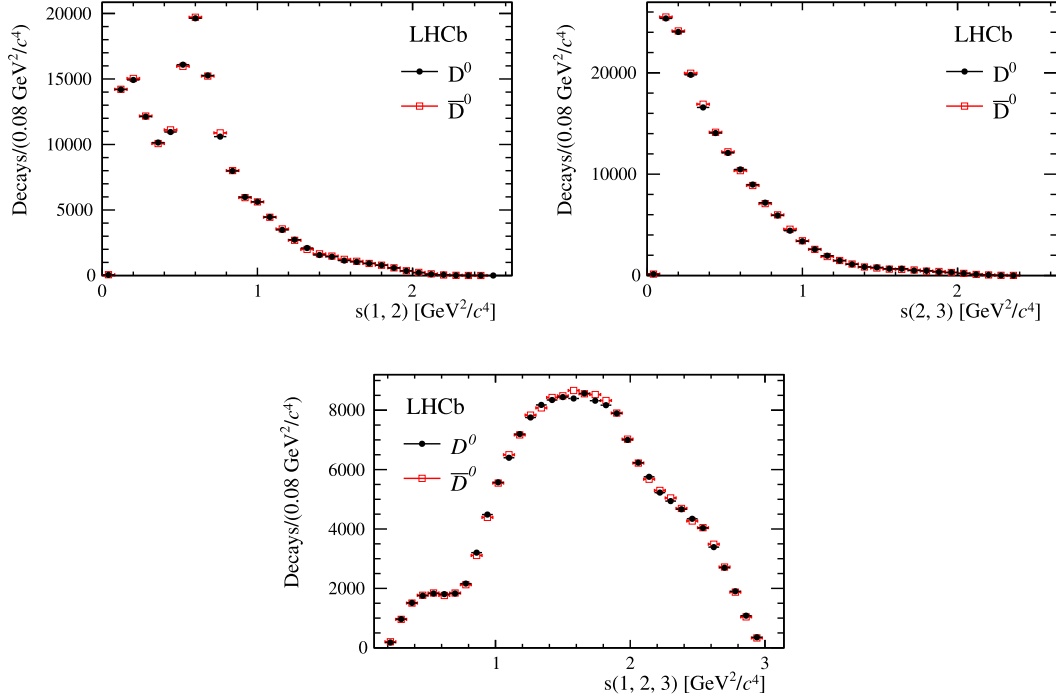


Fig. 3. Invariant mass-squared distributions for D^0 meson (black, closed circles) and \bar{D}^0 meson (red, open squares) decays to the final state $\pi^-\pi^+\pi^+\pi^-$. The invariant mass-squared combinations $s(1, 2)$, $s(2, 3)$, $s(1, 2, 3)$, $s(2, 3, 4)$, and $s(3, 4)$ correspond to $s(\pi^-, \pi^+)$, $s(\pi^+, \pi^+)$, $s(\pi^-, \pi^+, \pi^+)$, $s(\pi^+, \pi^+, \pi^-)$, and $s(\pi^+, \pi^-)$, respectively for the D^0 mode. The charge conjugate is taken for the \bar{D}^0 mode. Owing to the randomisation of the order of identical final-state particles the invariant mass-squared distributions $s(2, 3, 4)$ and $s(3, 4)$ are statistically compatible with the invariant mass-squared distributions $s(1, 2, 3)$ and $s(1, 2)$, respectively. As such the invariant mass-squared distributions $s(2, 3, 4)$ and $s(3, 4)$ are not shown. The phase-space distribution of the $D^0 \rightarrow \pi^-\pi^+\pi^+\pi^-$ decay is expected to be dominated by contributions from $D^0 \rightarrow a_1(1260)^+\pi^-$ and $D^0 \rightarrow \rho^0\rho^0$ decays [21]. (For interpretation of the references to colour in this figure legend, the reader is referred to the web version of this Letter.)

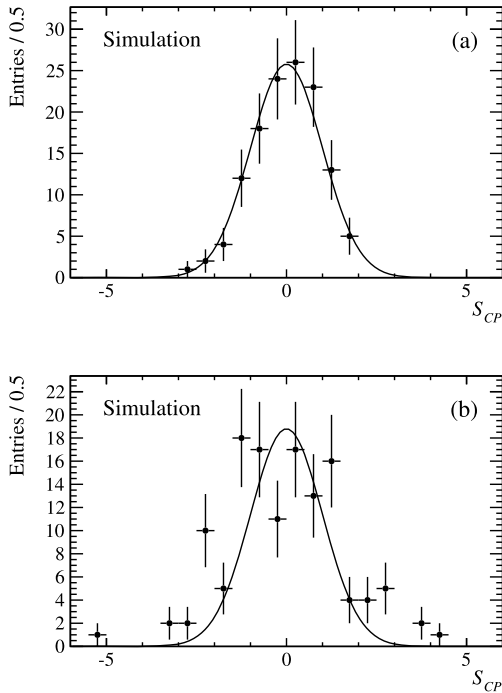


Fig. 4. Distributions of S_{CP} for (a) a typical pseudo-experiment with generated $D^0 \rightarrow \pi^-\pi^+\pi^+\pi^-$ decays without CPV and for (b) a typical pseudo-experiment with a generated 10° phase difference between $D^0 \rightarrow a_1(1260)^+\pi^-$ and $\bar{D}^0 \rightarrow a_1(1260)^-\pi^+$ resonant decays. The points show the data distribution and the solid line is a reference Gaussian distribution corresponding to the no CPV hypothesis. The corresponding p -values under the hypothesis of no asymmetry for (a) decays without CPV and (b) decays with a 10° phase difference between $D^0 \rightarrow a_1(1260)^+\pi^-$ and $\bar{D}^0 \rightarrow a_1(1260)^-\pi^+$ resonant components are 85.6% and 1.1×10^{-16} , respectively.

each with approximately 2500 signal events is chosen for $D^0 \rightarrow \pi^-\pi^+\pi^+\pi^-$ decays. The p -values for the pseudo-experiments are uniformly distributed for the case of no CPV. The average p -value for a pseudo-experiment with a phase difference of 10° or a magnitude difference of 10% between $D^0 \rightarrow \phi\rho^0$ and $\bar{D}^0 \rightarrow \phi\rho^0$ decays for the $D^0 \rightarrow K^-K^+\pi^-\pi^+$ mode and between $D^0 \rightarrow a_1(1260)^+\pi^-$ and $\bar{D}^0 \rightarrow a_1(1260)^-\pi^+$ decays for the $D^0 \rightarrow \pi^-\pi^+\pi^+\pi^-$ mode is below 10^{-3} .

7. Results

Asymmetries are searched for in the $D^0 \rightarrow K^-\pi^+\pi^+\pi^-$ control channel. The distributions of S_{CP} and local CP asymmetry, defined as

$$A_{CP}^i = \frac{N_i(D^0) - \alpha N_i(\bar{D}^0)}{N_i(D^0) + \alpha N_i(\bar{D}^0)}, \quad (4)$$

are shown in Fig. 5 for the $D^0 \rightarrow K^-\pi^+\pi^+\pi^-$ control channel. The data set is also studied to identify sources of asymmetry with two alternative partitions and by separating data taken with each magnet polarity. The results, displayed in Table 1, show that no asymmetry is observed in $D^0 \rightarrow K^-\pi^+\pi^+\pi^-$ decays. Furthermore, the data sample is split into 10 time-ordered samples of approximately equal size, for each polarity. The p -values under the hypothesis of no asymmetry are uniformly distributed across the data taking period. No evidence for a significant asymmetry in any bin is found.

The S_{CP} and local CP asymmetry distributions for $D^0 \rightarrow K^-K^+\pi^-\pi^+$ decays for a partition containing 32 bins and for $D^0 \rightarrow \pi^-\pi^+\pi^+\pi^-$ decays with a partition containing 128 bins are shown in Fig. 5. The p -values under the hypothesis of no CP violation for the decays $D^0 \rightarrow K^-K^+\pi^-\pi^+$ and $D^0 \rightarrow \pi^-\pi^+\pi^+\pi^-$ are 9.1% and 41%, respectively, the corresponding χ^2/ndf s are

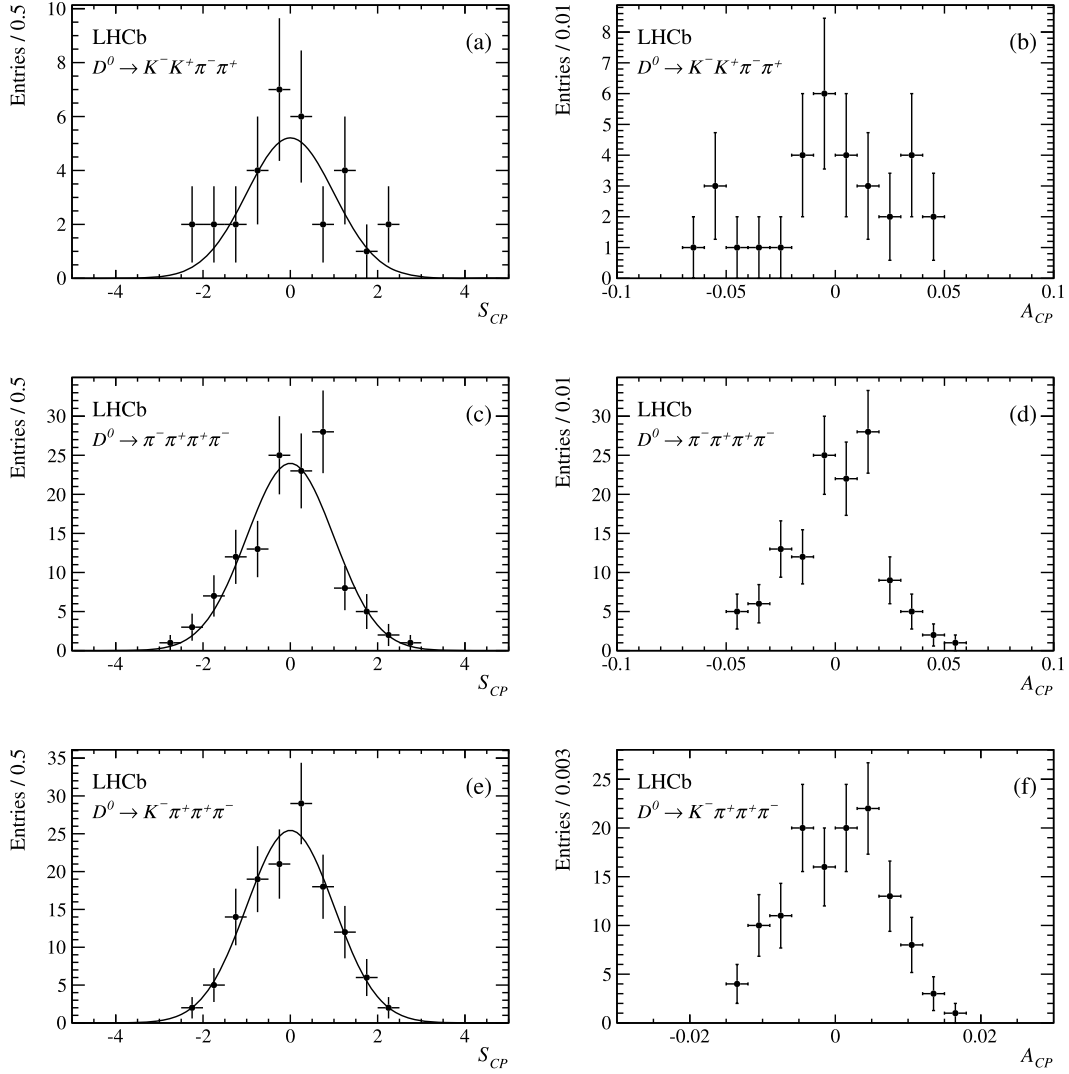


Fig. 5. Distributions of (a), (c), (e) S_{CP} and (b), (d), (f) local CP asymmetry per bin for (a), (b) $D^0 \rightarrow K^- K^+ \pi^- \pi^+$ decays partitioned with 32 bins, for (c), (d) $D^0 \rightarrow \pi^- \pi^+ \pi^+ \pi^-$ decays partitioned with 128 bins, and for (e), (f) the control channel $D^0 \rightarrow K^- \pi^+ \pi^+ \pi^-$ partitioned with 128 bins. The points show the data distribution and the solid line is a reference Gaussian distribution corresponding to the no CPV hypothesis.

Table 1

The χ^2/ndf and p -values under the hypothesis of no CPV for the control channel $D^0 \rightarrow K^- \pi^+ \pi^+ \pi^-$. The p -values are calculated separately for data samples taken with magnet up polarity, magnet down polarity, and the two polarities combined.

Bins	p -Value (%) (χ^2/ndf) Magnet down	p -Value (%) (χ^2/ndf) Magnet up	p -Value (%) (χ^2/ndf) Combined sample
16	80.8 (10.2/15)	21.2 (19.1/15)	34.8 (16.5/15)
128	62.0 (121.5/127)	75.9 (115.5/127)	80.0 (113.4/127)
1024	27.5 (1049.6/1023)	9.9 (1081.6/1023)	22.1 (1057.5/1023)

Table 2

The p -values and χ^2/ndf under the hypothesis of no CPV with the default partitions for $D^0 \rightarrow K^- K^+ \pi^- \pi^+$ decays and $D^0 \rightarrow \pi^- \pi^+ \pi^+ \pi^-$ decays. The p -values are calculated for a combined data sample with both data taken with magnet up polarity and data taken with magnet down polarity.

Channel	Bins	p -Value (%)	χ^2/ndf
$D^0 \rightarrow K^- K^+ \pi^- \pi^+$	32	9.1	42.0/31
$D^0 \rightarrow \pi^- \pi^+ \pi^+ \pi^-$	128	41.0	130.0/127

shown in Table 2. The consistency of the result is checked with alternative partitions, shown in Table 3. In each case the result is consistent with the no CPV hypothesis.

Table 3

The p -values and χ^2/ndf under the hypothesis of no CPV with two alternative partitions for $D^0 \rightarrow K^- K^+ \pi^- \pi^+$ decays and $D^0 \rightarrow \pi^- \pi^+ \pi^+ \pi^-$ decays. The p -values are calculated for a combined data sample with both data taken with magnet up polarity and data taken with magnet down polarity.

Channel	Bins	p -Value (%)	χ^2/ndf
$D^0 \rightarrow K^- K^+ \pi^- \pi^+$	16	9.1	22.7/15
	64	13.1	75.7/63
$D^0 \rightarrow \pi^- \pi^+ \pi^+ \pi^-$	64	28.8	68.8/63
	256	61.7	247.7/255

The stability of the results is checked for each polarity in 10 approximately equal-sized, time-ordered data samples. The p -values are uniformly distributed across the 2011 data taking period and are consistent with the no CPV hypothesis.

8. Conclusions

A model-independent search for CPV in 5.7×10^4 $D^0 \rightarrow K^- K^+ \pi^- \pi^+$ decays and 3.3×10^5 $D^0 \rightarrow \pi^- \pi^+ \pi^+ \pi^-$ decays is presented. The analysis is sensitive to CPV that would arise from a phase difference of $\mathcal{O}(10^\circ)$ or a magnitude difference

of $\mathcal{O}(10\%)$ between $D^0 \rightarrow \phi\rho^0$ and $\bar{D}^0 \rightarrow \phi\rho^0$ decays for the $D^0 \rightarrow K^-K^+\pi^-\pi^+$ mode and between $D^0 \rightarrow a_1(1260)^+\pi^-$ and $\bar{D}^0 \rightarrow a_1(1260)^-\pi^+$ decays for the $D^0 \rightarrow \pi^-\pi^+\pi^+\pi^-$ mode. For none of the 32 bins, each with approximately 1800 signal events, is an asymmetry greater than 6.5% observed for $D^0 \rightarrow K^-K^+\pi^-\pi^+$ decays, and for none of the 128 bins, each with approximately 2500 signal events, is an asymmetry greater than 5.5% observed for $D^0 \rightarrow \pi^-\pi^+\pi^+\pi^-$ decays. Assuming CP conservation, the probabilities to observe local asymmetries across the phase space of the D^0 meson decay as large or larger than those in data for the decays $D^0 \rightarrow K^-K^+\pi^-\pi^+$ and $D^0 \rightarrow \pi^-\pi^+\pi^+\pi^-$ are 9.1% and 41%, respectively. All results are consistent with CP conservation at the current sensitivity.

Acknowledgements

We express our gratitude to our colleagues in the CERN accelerator departments for the excellent performance of the LHC. We thank the technical and administrative staff at the LHCb institutes. We acknowledge support from CERN and from the national agencies: CAPES, CNPq, FAPERJ and FINEP (Brazil); NSFC (China); CNRS/IN2P3 and Region Auvergne (France); BMBF, DFG, HGF and MPG (Germany); SFI (Ireland); INFN (Italy); FOM and NWO (The Netherlands); SCSR (Poland); MEN/IFA (Romania); MinES, Rosatom, RFBR and NRC “Kurchatov Institute” (Russia); MinECo, XuntaGal and GENCAT (Spain); SNSF and SER (Switzerland); NAS Ukraine (Ukraine); STFC (United Kingdom); NSF (USA). We also acknowledge the support received from the ERC under FP7. The Tier1 computing centres are supported by IN2P3 (France), KIT and BMBF (Germany), INFN (Italy), NWO and SURF (The Netherlands), PIC (Spain), GridPP (United Kingdom). We are thankful for the computing resources put at our disposal by Yandex LLC (Russia), as well as to the communities behind the multiple open source software packages that we depend on.

Open access

This article is published Open Access at sciencedirect.com. It is distributed under the terms of the Creative Commons Attribution License 3.0, which permits unrestricted use, distribution, and reproduction in any medium, provided the original authors and source are credited.

LHCb Collaboration

R. Aaij⁴⁰, B. Adeva³⁶, M. Adinolfi⁴⁵, C. Adrover⁶, A. Affolder⁵¹, Z. Ajaltouni⁵, J. Albrecht⁹, F. Alessio³⁷, M. Alexander⁵⁰, S. Ali⁴⁰, G. Alkhazov²⁹, P. Alvarez Cartelle³⁶, A.A. Alves Jr.^{24,37}, S. Amato², S. Amerio²¹, Y. Amhis⁷, L. Anderlini^{17,f}, J. Anderson³⁹, R. Andreassen⁵⁶, J.E. Andrews⁵⁷, R.B. Appleby⁵³, O. Aquines Gutierrez¹⁰, F. Archilli¹⁸, A. Artamonov³⁴, M. Artuso⁵⁸, E. Aslanides⁶, G. Auriemma^{24,m}, M. Baalouch⁵, S. Bachmann¹¹, J.J. Back⁴⁷, C. Baesso⁵⁹, V. Balagura³⁰, W. Baldini¹⁶, R.J. Barlow⁵³, C. Barschel³⁷, S. Barsuk⁷, W. Barter⁴⁶, Th. Bauer⁴⁰, A. Bay³⁸, J. Beddow⁵⁰, F. Bedeschi²², I. Bediaga¹, S. Belogurov³⁰, K. Belous³⁴, I. Belyaev³⁰, E. Ben-Haim⁸, G. Bencivenni¹⁸, S. Benson⁴⁹, J. Benton⁴⁵, A. Berezhnoy³¹, R. Bernet³⁹, M.-O. Bettler⁴⁶, M. van Beuzekom⁴⁰, A. Bien¹¹, S. Bifani⁴⁴, T. Bird⁵³, A. Bizzeti^{17,h}, P.M. Bjørnstad⁵³, T. Blake³⁷, F. Blanc³⁸, J. Blouw¹¹, S. Blusk⁵⁸, V. Bocci²⁴, A. Bondar³³, N. Bondar²⁹, W. Bonivento¹⁵, S. Borghi⁵³, A. Borgia⁵⁸, T.J.V. Bowcock⁵¹, E. Bowen³⁹, C. Bozzi¹⁶, T. Brambach⁹, J. van den Brand⁴¹, J. Bressieux³⁸, D. Brett⁵³, M. Britsch¹⁰, T. Britton⁵⁸, N.H. Brook⁴⁵, H. Brown⁵¹, I. Burducea²⁸, A. Bursche³⁹, G. Busetto^{21,q}, J. Buytaert³⁷, S. Cadeddu¹⁵, O. Callot⁷, M. Calvi^{20,j}, M. Calvo Gomez^{35,n}, A. Camboni³⁵,

References

- [1] S. Bianco, F. Fabbri, D. Benson, I. Bigi, A Cicerone for the physics of charm, Riv. Nuovo Cimento 26 (7) (2003) 1, arXiv:hep-ex/0309021.
- [2] D.-S. Du, CP violation for neutral charmed meson decays into CP eigenstates, Eur. Phys. J. C 50 (2007) 579, arXiv:hep-ph/0608313.
- [3] F. Buccella, M. Lusignoli, A. Pugliese, P. Santorelli, CP violation in D meson decays: would it be a sign of new physics?, arXiv:1305.7343.
- [4] M. Bobrowski, A. Lenz, J. Riedl, J. Rohrwild, How large can the SM contribution to CP violation in $D^0 - \bar{D}^0$ mixing be?, J. High Energy Phys. 1003 (2010) 009, arXiv:1002.4794.
- [5] Y. Grossman, A.L. Kagan, Y. Nir, New physics and CP violation in singly Cabibbo suppressed D decays, Phys. Rev. D 75 (2007) 036008, arXiv:hep-ph/0609178.
- [6] A.A. Petrov, Searching for new physics with Charm, PoS BEAUTY 2009 (2009) 024, arXiv:1003.0906.
- [7] LHCb Collaboration, R. Aaij, et al., Search for direct CP violation in $D^0 \rightarrow h^-h^+$ modes using semileptonic B decays, Phys. Lett. B 723 (2013) 33, arXiv:1303.2614.
- [8] LHCb Collaboration, R. Aaij, et al., Searches for CP violation in the $D^+ \rightarrow \phi\pi^+$ and $D_s^+ \rightarrow K_S^0\pi^+$ decays, J. High Energy Phys. 1306 (2013) 112, arXiv:1303.4906.
- [9] LHCb Collaboration, R. Aaij, et al., Evidence for CP violation in time-integrated $D^0 \rightarrow h^-h^+$ decay rates, Phys. Rev. Lett. 108 (2012) 111602, arXiv:1112.0938.
- [10] CLEO Collaboration, M. Artuso, et al., Amplitude analysis of $D^0 \rightarrow K^+K^-\pi^+\pi^-$, Phys. Rev. D 85 (2012) 122002, arXiv:1201.5716.
- [11] I. Bediaga, et al., On a CP anisotropy measurement in the Dalitz plot, Phys. Rev. D 80 (2009) 096006, arXiv:0905.4233.
- [12] BaBar Collaboration, B. Aubert, et al., Search for CP violation in neutral D meson Cabibbo-suppressed three-body decays, Phys. Rev. D 78 (2008) 051102, arXiv:0802.4035.
- [13] LHCb Collaboration, R. Aaij, et al., Search for CP violation in $D^+ \rightarrow K^-K^+\pi^+$ decays, Phys. Rev. D 84 (2011) 112008, arXiv:1110.3970.
- [14] LHCb Collaboration, A.A. Alves Jr., et al., The LHCb detector at the LHC, JINST 3 (2008) S08005.
- [15] M. Adinolfi, et al., Performance of the LHCb RICH detector at the LHC, Eur. Phys. J. C 73 (2013) 2431, arXiv:1211.6759.
- [16] R. Aaij, et al., The LHCb trigger and its performance in 2011, JINST 8 (2013) P04022, arXiv:1211.3055.
- [17] W.D. Hulsbergen, Decay chain fitting with a Kalman filter, Nucl. Instrum. Methods A552 (2005) 566, arXiv:physics/0503191.
- [18] T. Skwarnicki, A study of the radiative cascade transitions between the Upsilon-prime and Upsilon resonances, PhD thesis, Institute of Nuclear Physics, Krakow, 1986, DESY-F31-86-02.
- [19] N.L. Johnson, Systems of frequency curves generated by methods of translation, Biometrika 36 (1949) 149.
- [20] M. Pivk, F.R. Le, Diberder, sPlot: a statistical tool to unfold data distributions, Nucl. Instrum. Methods A555 (2005) 356, arXiv:physics/0402083.
- [21] FOCUS Collaboration, J. Link, et al., Study of the $D^0 \rightarrow \pi^-\pi^+\pi^-\pi^+$ decay, Phys. Rev. D 75 (2007) 052003, arXiv:hep-ex/0701001.
- [22] Particle Data Group, J. Beringer, et al., Review of particle physics, Phys. Rev. D 86 (2012) 010001.

P. Campana^{18,37}, D. Campora Perez³⁷, A. Carbone^{14,c}, G. Carboni^{23,k}, R. Cardinale^{19,i},
 A. Cardini¹⁵, H. Carranza-Mejia⁴⁹, L. Carson⁵², K. Carvalho Akiba², G. Casse⁵¹,
 L. Castillo Garcia³⁷, M. Cattaneo³⁷, Ch. Cauet⁹, R. Cenci⁵⁷, M. Charles⁵⁴,
 Ph. Charpentier³⁷, P. Chen^{3,38}, N. Chiapolini³⁹, M. Chrzaszcz²⁵, K. Ciba³⁷, X. Cid Vidal³⁷,
 G. Ciezarek⁵², P.E.L. Clarke⁴⁹, M. Clemencic³⁷, H.V. Cliff⁴⁶, J. Closier³⁷, C. Coca²⁸,
 V. Coco⁴⁰, J. Cogan⁶, E. Cogneras⁵, P. Collins³⁷, A. Comerma-Montells³⁵, A. Contu^{15,37},
 A. Cook⁴⁵, M. Coombes^{45,*}, S. Coquereau⁸, G. Corti³⁷, B. Couturier³⁷, G.A. Cowan⁴⁹,
 E. Cowie⁴⁵, D.C. Craik⁴⁷, S. Cunliffe⁵², R. Currie⁴⁹, C. D'Ambrosio³⁷, P. David⁸,
 P.N.Y. David⁴⁰, A. Davis⁵⁶, I. De Bonis⁴, K. De Bruyn⁴⁰, S. De Capua⁵³, M. De Cian¹¹,
 J.M. De Miranda¹, L. De Paula², W. De Silva⁵⁶, P. De Simone¹⁸, D. Decamp⁴,
 M. Deckenhoff⁹, L. Del Buono⁸, N. Déléage⁴, D. Derkach⁵⁴, O. Deschamps⁵, F. Dettori⁴¹,
 A. Di Canto¹¹, H. Dijkstra³⁷, M. Dogaru²⁸, S. Donleavy⁵¹, F. Dordei¹¹, A. Dosil Suárez³⁶,
 D. Dossett⁴⁷, A. Dovbnya⁴², F. Dupertuis³⁸, P. Durante³⁷, R. Dzhelyadin³⁴, A. Dziurda²⁵,
 A. Dzyuba²⁹, S. Easo⁴⁸, U. Egede⁵², V. Egorychev³⁰, S. Eidelman³³, D. van Eijk⁴⁰,
 S. Eisenhardt⁴⁹, U. Eitschberger⁹, R. Ekelhof⁹, L. Eklund^{50,37}, I. El Rifai⁵, Ch. Elsasser³⁹,
 A. Falabella^{14,e}, C. Färber¹¹, G. Fardell⁴⁹, C. Farinelli⁴⁰, S. Farry⁵¹, D. Ferguson⁴⁹,
 V. Fernandez Albor³⁶, F. Ferreira Rodrigues¹, M. Ferro-Luzzi³⁷, S. Filippov³², M. Fiore¹⁶,
 C. Fitzpatrick³⁷, M. Fontana¹⁰, F. Fontanelli^{19,i}, R. Forty³⁷, O. Francisco², M. Frank³⁷,
 C. Frei³⁷, M. Frosini^{17,f}, S. Furcas²⁰, E. Furfaro^{23,k}, A. Gallas Torreira³⁶, D. Galli^{14,c},
 M. Gandelman², P. Gandini⁵⁸, Y. Gao³, J. Garofoli⁵⁸, P. Garosi⁵³, J. Garra Tico⁴⁶,
 L. Garrido³⁵, C. Gaspar³⁷, R. Gauld⁵⁴, E. Gersabeck¹¹, M. Gersabeck⁵³, T. Gershon^{47,37},
 Ph. Ghez⁴, V. Gibson⁴⁶, L. Giubega²⁸, V.V. Gligorov³⁷, C. Göbel⁵⁹, D. Golubkov³⁰,
 A. Golutvin^{52,30,37}, A. Gomes², P. Gorbounov^{30,37}, H. Gordon³⁷, C. Gotti²⁰,
 M. Grabalosa Gándara⁵, R. Graciani Diaz³⁵, L.A. Granado Cardoso³⁷, E. Graugés³⁵,
 G. Graziani¹⁷, A. Grecu²⁸, E. Greening⁵⁴, S. Gregson⁴⁶, P. Griffith⁴⁴, O. Grünberg⁶⁰,
 B. Gui⁵⁸, E. Gushchin³², Yu. Guz^{34,37}, T. Gys³⁷, C. Hadjivasiliou⁵⁸, G. Haefeli³⁸,
 C. Haen³⁷, S.C. Haines⁴⁶, S. Hall⁵², B. Hamilton⁵⁷, T. Hampson⁴⁵,
 S. Hansmann-Menzemer¹¹, N. Harnew⁵⁴, S.T. Harnew⁴⁵, J. Harrison⁵³, T. Hartmann⁶⁰,
 J. He³⁷, T. Head³⁷, V. Heijne⁴⁰, K. Hennessy⁵¹, P. Henrard⁵, J.A. Hernando Morata³⁶,
 E. van Herwijnen³⁷, M. Hess⁶⁰, A. Hicheur¹, E. Hicks⁵¹, D. Hill⁵⁴, M. Hoballah⁵,
 C. Hombach⁵³, P. Hopchev⁴, W. Hulsbergen⁴⁰, P. Hunt⁵⁴, T. Huse⁵¹, N. Hussain⁵⁴,
 D. Hutchcroft⁵¹, D. Hynds⁵⁰, V. Iakovenko⁴³, M. Idzik²⁶, P. Ilten¹², R. Jacobsson³⁷,
 A. Jaeger¹¹, E. Jans⁴⁰, P. Jaton³⁸, A. Jawahery⁵⁷, F. Jing³, M. John⁵⁴, D. Johnson⁵⁴,
 C.R. Jones⁴⁶, C. Joram³⁷, B. Jost³⁷, M. Kaballo⁹, S. Kandybei⁴², W. Kanso⁶, M. Karacson³⁷,
 T.M. Karbach³⁷, I.R. Kenyon⁴⁴, T. Ketel⁴¹, A. Keune³⁸, B. Khanji²⁰, O. Kochebina⁷,
 I. Komarov³⁸, R.F. Koopman⁴¹, P. Koppenburg⁴⁰, M. Korolev³¹, A. Kozlinskiy⁴⁰,
 L. Kravchuk³², K. Kreplin¹¹, M. Kreps⁴⁷, G. Krocker¹¹, P. Krokovny³³, F. Kruse⁹,
 M. Kucharczyk^{20,25,j}, V. Kudryavtsev³³, K. Kurek²⁷, T. Kvaratskheliya^{30,37}, V.N. La Thi³⁸,
 D. Lacarrere³⁷, G. Lafferty⁵³, A. Lai¹⁵, D. Lambert⁴⁹, R.W. Lambert⁴¹, E. Lanciotti³⁷,
 G. Lanfranchi¹⁸, C. Langenbruch³⁷, T. Latham⁴⁷, C. Lazzeroni⁴⁴, R. Le Gac⁶,
 J. van Leerdam⁴⁰, J.-P. Lees⁴, R. Lefèvre⁵, A. Leflat³¹, J. Lefrançois⁷, S. Leo²², O. Leroy⁶,
 T. Lesiak²⁵, B. Leverington¹¹, Y. Li³, L. Li Gioi⁵, M. Liles⁵¹, R. Lindner³⁷, C. Linn¹¹,
 B. Liu³, G. Liu³⁷, S. Lohn³⁷, I. Longstaff⁵⁰, J.H. Lopes², N. Lopez-March³⁸, H. Lu³,
 D. Lucchesi^{21,q}, J. Luisier³⁸, H. Luo⁴⁹, F. Machefert⁷, I.V. Machikhiliyan^{4,30}, F. Maciuc²⁸,
 O. Maev^{29,37}, S. Malde⁵⁴, G. Manca^{15,d}, G. Mancinelli⁶, J. Maratas⁵, U. Marconi¹⁴,
 P. Marino^{22,s}, R. Märki³⁸, J. Marks¹¹, G. Martellotti²⁴, A. Martens⁸, A. Martín Sánchez⁷,
 M. Martinelli⁴⁰, D. Martinez Santos⁴¹, D. Martins Tostes², A. Martynov³¹,
 A. Massafferri¹, R. Matev³⁷, Z. Mathe³⁷, C. Matteuzzi²⁰, E. Maurice⁶,
 A. Mazurov^{16,32,37,e}, J. McCarthy⁴⁴, A. McNab⁵³, R. McNulty¹², B. McKelley⁵¹,
 B. Meadows^{56,54}, F. Meier⁹, M. Meissner¹¹, M. Merk⁴⁰, D.A. Milanes⁸, M.-N. Minard⁴,
 J. Molina Rodriguez⁵⁹, S. Monteil⁵, D. Moran⁵³, P. Morawski²⁵, A. Mordà⁶,
 M.J. Morello^{22,s}, R. Mountain⁵⁸, I. Mous⁴⁰, F. Muheim⁴⁹, K. Müller³⁹, R. Muresan²⁸,

B. Muryn²⁶, B. Muster³⁸, P. Naik⁴⁵, T. Nakada³⁸, R. Nandakumar⁴⁸, I. Nasteva¹,
M. Needham⁴⁹, S. Neubert³⁷, N. Neufeld³⁷, A.D. Nguyen³⁸, T.D. Nguyen³⁸,
C. Nguyen-Mau^{38,o}, M. Nicol⁷, V. Niess⁵, R. Niet⁹, N. Nikitin³¹, T. Nikodem¹¹,
A. Nomerotski⁵⁴, A. Novoselov³⁴, A. Oblakowska-Mucha²⁶, V. Obraztsov³⁴, S. Oggero⁴⁰,
S. Ogilvy⁵⁰, O. Okhrimenko⁴³, R. Oldeman^{15,d}, M. Orlandea²⁸, J.M. Otalora Goicochea²,
P. Owen⁵², A. Oyanguren³⁵, B.K. Pal⁵⁸, A. Palano^{13,b}, T. Palczewski²⁷, M. Palutan¹⁸,
J. Panman³⁷, A. Papanestis⁴⁸, M. Pappagallo⁵⁰, C. Parkes⁵³, C.J. Parkinson⁵²,
G. Passaleva¹⁷, G.D. Patel⁵¹, M. Patel⁵², G.N. Patrick⁴⁸, C. Patrignani^{19,i},
C. Pavel-Nicorescu²⁸, A. Pazos Alvarez³⁶, A. Pellegrino⁴⁰, G. Penso^{24,l}, M. Pepe Altarelli³⁷,
S. Perazzini^{14,c}, E. Perez Trigo³⁶, A. Pérez-Calero Yzquierdo³⁵, P. Perret⁵,
M. Perrin-Terrin⁶, L. Pescatore⁴⁴, E. Pesen⁶¹, K. Petridis⁵², A. Petrolini^{19,i}, A. Phan⁵⁸,
E. Picatoste Olloqui³⁵, B. Pietrzyk⁴, T. Pilař⁴⁷, D. Pinci²⁴, S. Playfer⁴⁹, M. Plo Casasus³⁶,
F. Polci⁸, G. Polok²⁵, A. Poluektov^{47,33}, E. Polycarpo², A. Popov³⁴, D. Popov¹⁰,
B. Popovici²⁸, C. Potterat³⁵, A. Powell⁵⁴, J. Prisciandaro³⁸, A. Pritchard⁵¹, C. Prouve⁷,
V. Pugatch⁴³, A. Puig Navarro³⁸, G. Punzi^{22,r}, W. Qian⁴, J.H. Rademacker^{45,*},
B. Rakotomiamanana³⁸, M.S. Rangel², I. Raniuk⁴², N. Rauschmayr³⁷, G. Raven⁴¹,
S. Redford⁵⁴, M.M. Reid⁴⁷, A.C. dos Reis¹, S. Ricciardi⁴⁸, A. Richards⁵², K. Rinnert⁵¹,
V. Rives Molina³⁵, D.A. Roa Romero⁵, P. Robbe⁷, D.A. Roberts⁵⁷, E. Rodrigues⁵³,
P. Rodriguez Perez³⁶, S. Roiser³⁷, V. Romanovsky³⁴, A. Romero Vidal³⁶, J. Rouvinet³⁸,
T. Ruf³⁷, F. Ruffini²², H. Ruiz³⁵, P. Ruiz Valls³⁵, G. Sabatino^{24,k}, J.J. Saborido Silva³⁶,
N. Sagidova²⁹, P. Sail⁵⁰, B. Saitta^{15,d}, V. Salustino Guimaraes², B. Sanmartin Sedes³⁶,
M. Sannino^{19,i}, R. Santacesaria²⁴, C. Santamarina Rios³⁶, E. Santovetti^{23,k}, M. Sapunov⁶,
A. Sarti^{18,l}, C. Satriano^{24,m}, A. Satta²³, M. Savrie^{16,e}, D. Savrina^{30,31}, P. Schaack⁵²,
M. Schiller⁴¹, H. Schindler³⁷, M. Schlupp⁹, M. Schmelling¹⁰, B. Schmidt³⁷,
O. Schneider³⁸, A. Schopper³⁷, M.-H. Schune⁷, R. Schwemmer³⁷, B. Sciascia¹⁸,
A. Sciubba²⁴, M. Seco³⁶, A. Semennikov³⁰, K. Senderowska²⁶, I. Sepp⁵², N. Serra³⁹,
J. Serrano⁶, P. Seyfert¹¹, M. Shapkin³⁴, I. Shapoval^{16,42}, P. Shatalov³⁰, Y. Shcheglov²⁹,
T. Shears^{51,37}, L. Shekhtman³³, O. Shevchenko⁴², V. Shevchenko³⁰, A. Shires⁹,
R. Silva Coutinho⁴⁷, M. Sirendi⁴⁶, N. Skidmore⁴⁵, T. Skwarnicki⁵⁸, N.A. Smith⁵¹,
E. Smith^{54,48}, J. Smith⁴⁶, M. Smith⁵³, M.D. Sokoloff⁵⁶, F.J.P. Soler⁵⁰, F. Soomro³⁸,
D. Souza⁴⁵, B. Souza De Paula², B. Spaan⁹, A. Sparkes⁴⁹, P. Spradlin⁵⁰, F. Stagni³⁷,
S. Stahl¹¹, O. Steinkamp³⁹, S. Stevenson⁵⁴, S. Stoica²⁸, S. Stone⁵⁸, B. Storaci³⁹,
M. Straticiuc²⁸, U. Straumann³⁹, V.K. Subbiah³⁷, L. Sun⁵⁶, S. Swientek⁹, V. Syropoulos⁴¹,
M. Szczekowski²⁷, P. Szczypka^{38,37}, T. Szumlak²⁶, S. T'Jampens⁴, M. Teklishyn⁷,
E. Teodorescu²⁸, F. Teubert³⁷, C. Thomas⁵⁴, E. Thomas³⁷, J. van Tilburg¹¹, V. Tisserand⁴,
M. Tobin³⁸, S. Tolk⁴¹, D. Tonelli³⁷, S. Topp-Joergensen⁵⁴, N. Torr⁵⁴, E. Tournefier^{4,52},
S. Tourneur³⁸, M.T. Tran³⁸, M. Tresch³⁹, A. Tsaregorodtsev⁶, P. Tsopelas⁴⁰, N. Tuning⁴⁰,
M. Ubeda Garcia³⁷, A. Ukleja²⁷, D. Urner⁵³, A. Ustyuzhanin^{52,p}, U. Uwer¹¹, V. Vagnoni¹⁴,
G. Valenti¹⁴, A. Vallier⁷, M. Van Dijk⁴⁵, R. Vazquez Gomez¹⁸, P. Vazquez Regueiro³⁶,
C. Vázquez Sierra³⁶, S. Vecchi¹⁶, J.J. Velthuis⁴⁵, M. Veltri^{17,g}, G. Veneziano³⁸,
M. Vesterinen³⁷, B. Viaud⁷, D. Vieira², X. Vilasis-Cardona^{35,n}, A. Vollhardt³⁹,
D. Volyanskyy¹⁰, D. Voong⁴⁵, A. Vorobyev²⁹, V. Vorobyev³³, C. Voß⁶⁰, H. Voss¹⁰,
R. Waldi⁶⁰, C. Wallace⁴⁷, R. Wallace¹², S. Wandernoth¹¹, J. Wang⁵⁸, D.R. Ward⁴⁶,
N.K. Watson⁴⁴, A.D. Webber⁵³, D. Websdale⁵², M. Whitehead⁴⁷, J. Wicht³⁷,
J. Wiechczynski²⁵, D. Wiedner¹¹, L. Wiggers⁴⁰, G. Wilkinson⁵⁴, M.P. Williams^{47,48},
M. Williams⁵⁵, F.F. Wilson⁴⁸, J. Wimberley⁵⁷, J. Wishahi⁹, W. Wislicki²⁷, M. Witek²⁵,
S.A. Wotton⁴⁶, S. Wright⁴⁶, S. Wu³, K. Wyllie³⁷, Y. Xie^{49,37}, Z. Xing⁵⁸, Z. Yang³,
R. Young⁴⁹, X. Yuan³, O. Yushchenko³⁴, M. Zangoli¹⁴, M. Zavertyaev^{10,a}, F. Zhang³,
L. Zhang⁵⁸, W.C. Zhang¹², Y. Zhang³, A. Zhelezov¹¹, A. Zhokhov³⁰, L. Zhong³,
A. Zvyagin³⁷

¹ Centro Brasileiro de Pesquisas Físicas (CBPF), Rio de Janeiro, Brazil² Universidade Federal do Rio de Janeiro (UFRJ), Rio de Janeiro, Brazil³ Center for High Energy Physics, Tsinghua University, Beijing, China

- ⁴ LAPP, Université de Savoie, CNRS/IN2P3, Annecy-Le-Vieux, France
⁵ Clermont Université, Université Blaise Pascal, CNRS/IN2P3, LPC, Clermont-Ferrand, France
⁶ CPPM, Aix-Marseille Université, CNRS/IN2P3, Marseille, France
⁷ LAL, Université Paris-Sud, CNRS/IN2P3, Orsay, France
⁸ LPNHE, Université Pierre et Marie Curie, Université Paris Diderot, CNRS/IN2P3, Paris, France
⁹ Fakultät Physik, Technische Universität Dortmund, Dortmund, Germany
¹⁰ Max-Planck-Institut für Kernphysik (MPIK), Heidelberg, Germany
¹¹ Physikalisches Institut, Ruprecht-Karls-Universität Heidelberg, Heidelberg, Germany
¹² School of Physics, University College Dublin, Dublin, Ireland
¹³ Sezione INFN di Bari, Bari, Italy
¹⁴ Sezione INFN di Bologna, Bologna, Italy
¹⁵ Sezione INFN di Cagliari, Cagliari, Italy
¹⁶ Sezione INFN di Ferrara, Ferrara, Italy
¹⁷ Sezione INFN di Firenze, Firenze, Italy
¹⁸ Laboratori Nazionali dell'INFN di Frascati, Frascati, Italy
¹⁹ Sezione INFN di Genova, Genova, Italy
²⁰ Sezione INFN di Milano Bicocca, Milano, Italy
²¹ Sezione INFN di Padova, Padova, Italy
²² Sezione INFN di Pisa, Pisa, Italy
²³ Sezione INFN di Roma Tor Vergata, Roma, Italy
²⁴ Sezione INFN di Roma La Sapienza, Roma, Italy
²⁵ Henryk Niewodniczanski Institute of Nuclear Physics Polish Academy of Sciences, Kraków, Poland
²⁶ AGH – University of Science and Technology, Faculty of Physics and Applied Computer Science, Kraków, Poland
²⁷ National Center for Nuclear Research (NCBJ), Warsaw, Poland
²⁸ Horia Hulubei National Institute of Physics and Nuclear Engineering, Bucharest-Magurele, Romania
²⁹ Petersburg Nuclear Physics Institute (PNPI), Gatchina, Russia
³⁰ Institute of Theoretical and Experimental Physics (ITEP), Moscow, Russia
³¹ Institute of Nuclear Physics, Moscow State University (SINP MSU), Moscow, Russia
³² Institute for Nuclear Research of the Russian Academy of Sciences (INR RAN), Moscow, Russia
³³ Budker Institute of Nuclear Physics (SB RAS) and Novosibirsk State University, Novosibirsk, Russia
³⁴ Institute for High Energy Physics (IHEP), Protvino, Russia
³⁵ Universitat de Barcelona, Barcelona, Spain
³⁶ Universidad de Santiago de Compostela, Santiago de Compostela, Spain
³⁷ European Organization for Nuclear Research (CERN), Geneva, Switzerland
³⁸ Ecole Polytechnique Fédérale de Lausanne (EPFL), Lausanne, Switzerland
³⁹ Physik-Institut, Universität Zürich, Zürich, Switzerland
⁴⁰ Nikhef National Institute for Subatomic Physics, Amsterdam, The Netherlands
⁴¹ Nikhef National Institute for Subatomic Physics and VU University Amsterdam, Amsterdam, The Netherlands
⁴² NSC Kharkiv Institute of Physics and Technology (NSC KIPT), Kharkiv, Ukraine
⁴³ Institute for Nuclear Research of the National Academy of Sciences (KINR), Kyiv, Ukraine
⁴⁴ University of Birmingham, Birmingham, United Kingdom
⁴⁵ H.H. Wills Physics Laboratory, University of Bristol, Bristol, United Kingdom
⁴⁶ Cavendish Laboratory, University of Cambridge, Cambridge, United Kingdom
⁴⁷ Department of Physics, University of Warwick, Coventry, United Kingdom
⁴⁸ STFC Rutherford Appleton Laboratory, Didcot, United Kingdom
⁴⁹ School of Physics and Astronomy, University of Edinburgh, Edinburgh, United Kingdom
⁵⁰ School of Physics and Astronomy, University of Glasgow, Glasgow, United Kingdom
⁵¹ Oliver Lodge Laboratory, University of Liverpool, Liverpool, United Kingdom
⁵² Imperial College London, London, United Kingdom
⁵³ School of Physics and Astronomy, University of Manchester, Manchester, United Kingdom
⁵⁴ Department of Physics, University of Oxford, Oxford, United Kingdom
⁵⁵ Massachusetts Institute of Technology, Cambridge, MA, United States
⁵⁶ University of Cincinnati, Cincinnati, OH, United States
⁵⁷ University of Maryland, College Park, MD, United States
⁵⁸ Syracuse University, Syracuse, NY, United States
⁵⁹ Pontifícia Universidade Católica do Rio de Janeiro (PUC-Rio), Rio de Janeiro, Brazil[†]
⁶⁰ Institut für Physik, Universität Rostock, Rostock, Germany[‡]
⁶¹ Celal Bayar University, Manisa, Turkey[‡]

* Corresponding authors.

^a P.N. Lebedev Physical Institute, Russian Academy of Science (LPI RAS), Moscow, Russia.

^b Università di Bari, Bari, Italy.

^c Università di Bologna, Bologna, Italy.

^d Università di Cagliari, Cagliari, Italy.

^e Università di Ferrara, Ferrara, Italy.

^f Università di Firenze, Firenze, Italy.

^g Università di Urbino, Urbino, Italy.

^h Università di Modena e Reggio Emilia, Modena, Italy.

ⁱ Università di Genova, Genova, Italy.

^j Università di Milano Bicocca, Milano, Italy.

^k Università di Roma Tor Vergata, Roma, Italy.

^l Università di Roma La Sapienza, Roma, Italy.

^m Università della Basilicata, Potenza, Italy.

ⁿ LIFAELS, La Salle, Universitat Ramon Llull, Barcelona, Spain.

^o Hanoi University of Science, Hanoi, Viet Nam.

^p Institute of Physics and Technology, Moscow, Russia.

^q Università di Padova, Padova, Italy.

^r Università di Pisa, Pisa, Italy.

^s Scuola Normale Superiore, Pisa, Italy.

^t Associated to: Universidade Federal do Rio de Janeiro (UFRJ), Rio de Janeiro, Brazil.

^u Associated to: Physikalisches Institut, Ruprecht-Karls-Universität Heidelberg, Heidelberg, Germany.

^v Associated to: European Organization for Nuclear Research (CERN), Geneva, Switzerland.